RSC Advances

ROYAL SOCIETY OF CHEMISTRY

www.rsc.org/advances

ULTRASONIC DECROSSLINKING OF CROSSLINKED HIGH-DENSITY POLYETHYLENE: EFFECT OF DEGREE OF CROSSLINKING

*Keyuan Huang and Avraam I. Isayev**

Department of Polymer Engineering, The University of Akron, Akron, OH 44325-0301

*Corresponding author: aisayev@uakron.edu

Abstract

Decrosslinking of peroxide crosslinked high-density polyethylene (XHDPE) of different degrees of crosslinking by means of an ultrasonic single-screw extruder (SSE) is investigated. Barrel pressure and ultrasonic power consumption during extrusion are recorded. Swelling test, rheological test, infrared spectroscopy, thermal analysis and tensile test are used to elucidate the structure-property relationship of decrosslinked XHDPE. It was found that a more intensive rupture of the crosslinked network occurs in XHDPE of higher degree of crosslinking. Analysis based on the Horikx function shows that the type of preferential bond breakage during decrosslinking of XHDPE of various degrees of crosslinking is not determined by the bond energy alone but also influenced by structural characteristics of the network. The activation energy of viscous flow of sols extracted from various decrosslinked XHDPEs supports the analysis based on the Horikx function. The dynamic, thermal and tensile properties of the decrosslinked XHDPE are greatly affected by the type of preferential bond breakage. A significant improvement in the processibility and mechanical properties of decrosslinked 2% peroxide cured XHDPE is achieved due to the occurrence of a highly preferential breakage of crosslinks during ultrasonic decrosslinking.

Introduction

Recycling of crosslinked PE (XPE) is a challenge for the plastic industry due to the presence of the crosslinked three dimensional network. An ideal method to reprocess the XPE is to preferentially break crosslinks without breaking main chains in order to maintain the mechanical properties of the decrosslinked XPE. In the peroxide and irradiation crosslinked PE, the crosslinks and main chains are all carbon-carbon bonds. Therefore, the preferential breakage of crosslinks is difficult [1]. Thus, in the present context the decrosslinking or partial decrosslinking of peroxide and irradiation crosslinked PE is considered as a process to obtain a melt processible polymer exhibiting the desirable rheological behavior and mechanical performance. Various studies [1-7] are dedicated to decrosslinking of XPE. However, most of them [2-7] have not discussed the issue related to the type of bond breakage during decrosslinking of XPE.

The ultrasonic batch reactor and ultrasonic extruder were used to devulcanize various rubber vulcanizates [8-13] and decrosslink XHDPE [14, 15]. The analysis of the gel fraction-crosslink density relationship of various ultrasonically devulcanized rubbers showed that the ultrasound may induce a preferential breakage of crosslinks [10-13]. This is due to the difference in bond energy of the chemical bonds in the main chains and the crosslinks. Therefore, the preferential breakage of crosslinks cannot be achieved during decrosslinking of the peroxide and irradiation crosslinked PE, since the crosslinks and main chains are all carbon-carbon bonds.

The present study is aimed to investigate the effect of the degree of crosslinking of XHDPE on its ultrasonic decrosslinking using SSE. The process characteristics, structural, rheological and mechanical properties of these decrosslinked XHDPEs are studied. The type of bond breakage during the ultrasonic decrosslinking of XHDPE is revealed and structural factors governing this process are found. These findings provide fundamental understanding of the ultrasonic decrosslinking process of XHDPE leading to a possibility to obtain the decrosslinked XHDPE with superior mechanical properties.

Experimental

Materials

HDPE used was a rotational molding grade, 35 mesh powder (Paxon 7004, Exxon Mobil, Baytown, TX). Crosslinking agent was dicumyl peroxide in the pellet form (DC-40, Akrochem, Akron, OH). It contains 40 wt% peroxide and 60 wt% calcium carbonate as a carrier. Tetrakis [methylene (3,5-di-tert-butyl-4-hydroxyhydro cinnamate)] methane (Antioxidant 1010, Akrochem, Akron, OH) was used as a stabilizer during the rheological test. Xylene (mixture of isomers, ACS Reagent Grade, Sigma-Aldrich, WI) was used as a solvent for the swelling test. Hexane (ACS Reagent Grade, J.T. Baker, Pittsburgh, PA) was used to precipitate the dissolved sol from xylene. The sol was the soluble fraction of samples in the swelling test.

Three concentrations of peroxide DC-40 (2.5, 5.0 and 10.0 wt%) were used to prepare XHDPE of different degrees of crosslinking corresponding to active peroxide contents of 1.0, 2.0 and 4.0 wt%, respectively. Accordingly, these samples are called 1%, 2% and 4% XHDPE. The mixture of HDPE powder and DC-40 pellets are homogenized by a high speed mixer using the procedure employed earlier [15].

XHDPE slabs of three levels of crosslink density of dimensions of 26 cm x 26 cm x 1.25 cm were produced by a compression molding press (Carver, Wabash, IN) at a hydraulic pressure of 50 MPa and a temperature of 180^{o}C for 30 min, 20 min and 15 min, respectively. The reaction time was determined by performing the curing test by means of the Advanced Polymer Analyzer (APA 2000, Alpha Technology, Akron, OH). The obtained XHDPE slabs were crushed by a grinder (WSL180/180, Weima, Fort Mill, SC) with sieve having holes of a diameter of 4.5 mm. It was confirmed that the grinding process has no effect on the gel fraction of XHDPE.

Ultrasonic decrosslinking of the XHDPE

A 25.4 mm ultrasonic SSE (KL 100, L/D=33, Killion Corporation, Riviera Beach, FL) equipped with a circular die of a diameter of 2 mm and a length of 60.5 mm was employed. The schematic design of the ultrasonic SSE and the photograph of the screw are given in Figure 1 (a) and Figure 1 (b), respectively. The SSE was equipped with two boosters and converters connected to two water-cooled ultrasonic horns operating at a frequency of 20 kHz. Screw contains two mixing sections including the Union Carbide Mixer (UCM) and the melt star mixer

as shown in Figure 1b. More details about the extruder can be found from the previous study [15]. Ultrasonic decrosslinking of the 1% and 2% XHDPE by means of SSE with the die was performed at a flow rate of 7.5 g/min and ultrasonic amplitudes of 5, 7.5 and 10 μm. The mean residence time in the ultrasonic treatment zone at this flow rate was 15.5 s. Also, decrosslinking of the 1% and 2% XHDPE without imposition of ultrasound was performed on the same SSE. The extrusion of the 4% XHDPE at this flow rate without and with ultrasonic treatment at amplitudes of 5 and 7.5 μm cannot be performed due to an excessive torque. Thus, the ultrasonic decrosslinking of 4% XHDPE was carried out using the SSE without die at these processing conditions. Also, ultrasonic decrosslinking at an amplitude of 10 μm was carried out on the SSE with and without the die. The temperature of barrel and die are set up at 200^{o}C and temperature of feed port zone is 180^{o}C. The barrel pressure before the ultrasonic treatment zone and the ultrasonic power consumption were recorded. All other procedures and equipments were same as in earlier study [15].

Preparation of Specimens and Their Characterization

The compression molded sheets of decrosslinked XHDPE of 34 cm x 16 cm x 0.185 cm were prepared at a temperature of 200^{o}C and a pressure of 50 MPa for 20 mins. However, the decrosslinked 4% XHDPE without ultrasonic treatment cannot be molded into a sheet due to its insufficient flowability.

Swelling test of XHDPE and decrosslinked XHDPE was performed by following ASTM D 2765, test method C. The crosslink density of XHDPE and decrosslinked XHDPE was determined by Flory-Rehner equation [16].

A Fourier Transform Infrared Spectrometer (Nicolet 380, Thermo Scientific Corporation, Waltham, MA) was employed to obtain the FTIR spectra in the range of 525-4000 cm^{-1} with 32 consecutive scans at a resolution of 2 cm^{-1} in the reflective mode. The spectra of the compression molded sheets of the XHDPE and decrosslinked XHDPE obtained at an amplitude of 10 μm is obtained to investigate their chemical structure.

Small amplitude oscillatory shear (SAOS) test of XHDPE and decrosslinked XHDPE at a temperature of 160^{o}C was performed by using a stress controlled Discover Hybrid Rheometer

(DHR-2, TA Instruments, New Castle, DE) equipped with 25 mm parallel plates. A circular disk of a diameter of 25 mm was cut from the compression molded sheet. A gap of 2 mm was used for the test. By measuring dynamic properties at different gaps (2 mm and 1.5 mm), it was proven that no slippage occurred during the test [17]. The frequency sweep was in the range from 0.1 to 100 rad/s at a stress amplitude of 500 Pa. SAOS test of HDPE, the sol of XHDPE and decrosslinked XHDPE at temperatures of 140, 150 and 160^{o}C was also performed to calculate the activation energy for flow. Due to the limited amount of sol, a 25 mm circular disk of a thickness of 0.3 mm was used. For HDPE and sols of decrosslinked 1% and 2% XHDPE, the frequency sweep was in the range from 0.5 to 79 rad/s at a shear stress amplitude of 250 Pa. Due to the low viscosity of sol of decrosslinked 4% XHDPE, the frequency sweep was in the same frequency range but at a stress amplitude of 20 Pa. It was confirmed that these stress amplitudes were within the linear region. All the SAOS tests were repeated twice with the difference being less than 5%.

Differential Scanning Calorimetry (DSC, Model Q200, TA Instruments, New Castle, DE) was used to investigate the thermal behavior of HDPE, XHDPE and decrosslinked XHDPE. Samples were cut from tensile specimens by a stainless steel one sided razor blade. The cut samples of about 10 mg were sealed into the DSC hermetic pans (PS 1007, PS 1010, Instrument Specialist Inc., Twin Lakes, WI). To remove the thermal history, the heating-cooling-heating cycle at a rate of 10°C/min was applied in nitrogen environment. Samples were heated from 40 to 200°C, maintained at 200°C for 10 min, cooled from 200 to 40°C and equilibrated at 40°C, and finally heated from 40 to 200°C. The melting temperature and enthalpy were calculated from the second heating. The melting enthalpy of 282 J/mol of the perfect linear PE crystal [18] was used to evaluate the crystallinity. The reported crystallinity and melting temperature are the average value of at least two measurements.

Tensile test was performed by using an Instron tensile tester (Mode 5567, Instron, Canton, MA) at a crosshead speed of 25 mm/min without an extensometer. Dumbbell shape tensile test specimens were cut from the compression molded sheet by using a cutting die of a width of 5 mm and a gauge length of 23 mm. The stress-strain curves were recorded by a computer and used to calculate the Young's modulus, yield stress, stress and strain at break. The error bars were calculated as the standard deviation of at least 5 test results.

Results and Discussions

Barrel pressure and ultrasonic power consumption

Figure 2 shows the barrel pressure before ultrasonic treatment zone (a) and the ultrasonic power consumption (b) as a function of the ultrasonic amplitude during extrusion of XHDPE of various degrees of crosslinking at a flow rate of 7.5 g/min with or without the die. It is seen from Figure 1a that the barrel pressure with the die decreases with the amplitude and increases with the degree of crosslinking. The increase of the barrel pressure with the degree of crosslinking is a result of the increase of viscosity, as shown later. The decrease of the barrel pressure with the ultrasonic amplitude is due to both the thixotropic effect such as the shear thining and permanent effect including the decrease of the viscosity caused by the decrease of the gel fraction and crosslink density [10, 12, 15]. During extrusion of 4% XHDPE, the barrel pressure is significantly higher with the die than that without the die. This is due to the fact that the die increases the flow resistance during extrusion. Accordingly, a higher barrel pressure is needed in order for the screw to push the material through the die orifice.

It is seen from Figure 2b that the ultrasonic power consumption increases with the ultrasonic amplitude but shows a weak dependence on the degree of crosslinking during extrusion with the die. Also, the ultrasonic power consumption is lower without the die than that with the die during extrusion of 4% XHDPE. According to the simulation study of ultrasonic devulcanization of rubbers, the ultrasound can induce formation of bubbles [19] and cause their oscillation [20]. Therefore, the ultrasonic power consumption is a function of the hydrostatic pressure, acoustic pressure, sound velocity, loss tangent of material at an ultrasonic frequency of 20 kHz [20]. Clearly, the increase of the ultrasonic power consumption with the ultrasonic amplitude is due to the fact that the ultrasonic power consumption is proportional to the acoustic pressure which in turn is proportional to the amplitude. The weak dependence of the ultrasonic power consumption on the degree of crosslinking of XHDPE is most likely due to the sound velocity and loss tangent of XHDPE at the ultrasonic frequency is not significantly affected by the degree of crosslinking. The ultrasonic frequency used is within the rubbery plateau of HDPE. The study [21] showed that the dynamic properties of the uncrosslinked and crosslinked polybutadiene within its rubbery plateau were insignificantly affected by its degree of

crosslinking. Accordingly, the sound velocity and loss tangent of the XHDPE at the ultrasonic frequency is very likely insignificantly affected by the degree of crosslinking. Thus, it is not surprising to find a weak dependence of the ultrasonic power consumption on the degree of crosslinking of XHDPE. The lower ultrasonic power consumption during the ultrasonic extrusion of 4% XHDPE without the die than that with the die is due to the fact that the hydrostatic pressure (the barrel pressure in this case) is lower in the absence of the die. From the simulation studies, it is known that the ultrasonic power consumption decreases with the volume fraction of bubbles which is reduced with the hydrostatic pressure [20]. Thus, the ultrasonic power consumption increases with the barrel pressure.

Gel Fraction and Crosslink Density

Figure 3 shows gel fraction (a) and crosslink density (b) of decrosslinked XHDPE as a function of the ultrasonic amplitude. The gel fraction and crosslink density of XHDPE are also indicated. It is seen from Figure 3 that the gel fraction and crosslink density of XHDPE and decrosslinked XHDPE increases with the degree of crosslinking. The gel fraction and crosslink density of decrosslinked XHDPE without ultrasonic treatment is significantly lower than those of the corresponding XHDPE. This indicates that there is a substantial decrosslinking of XHDPE caused by stresses arising from screw rotation during extrusion of XHDPE. The ultrasonic treatment leads to a further decrease of the gel fraction and crosslink density of decrosslinked XHDPE with the effect increasing with the ultrasonic amplitude. It is also seen from Figure 3 that the gel fraction of the decrosslinked 4% XHDPE during extrusion with the die at an amplitude of 10 μm exhibits a lower gel fraction but a higher crosslink density than that without the die at the same amplitude. This is due to the higher barrel pressure with the die. However, the gel fraction and crosslink density of the decrosslinked 2% XHDPE obtained at an amplitude of 5 μm is slightly higher than that without ultrasonic treatment. This is possibly due to the nonlinear interaction between the mechanical and ultrasonic decrosslinking of XHDPE.

Since bonds in the crosslinks and main chains of XHDPE are all carbon-carbon bonds, the spectroscopic characterization can hardly distinguish their difference. Therefore, it is difficult to determine the type of preferential bond breakage during decrosslinking of XHDPE. Another method to determine the type of bond breakage is to apply certain statistical theories to analyze

the relationship between the gel fraction and crosslink density of decrosslinked XHDPE. Two theories are available. The first one is known as Horikx function [22] which is derived from the statistical theory dealing with the gel fraction-crosslink density relationship of the crosslinked linear polymers. The second one is Yashin and Isayev theory derived for the gel fraction-crosslink density relationship based on the rubber statistics theory [13] as proposed by Dobson and Gordon. However, the second theory can only be applied to highly crosslinked polymers and not applicable to 1% XHDPE of this study. Therefore, the following Horikx functions are used for the analysis in the present study:

$$1-\frac{\nu_{DXHDPE}}{\nu_{XHDPE}}=1-\frac{\left(1-\left(1-\zeta_{DXHDPE}\right)^{1/2}\right)^{2}}{\left(1-\left(1-\zeta_{XHDPE}\right)^{1/2}\right)^{2}} \quad (1)$$

$$1-\frac{\nu_{DXHDPE}}{\nu_{XHDPE}}=1-\frac{\left(M_n\times\nu_{DXHDPE}+2\right)\left(1-\left(1-\zeta_{DXHDPE}\right)^{1/2}\right)^{2}}{\left(M_n\times\nu_{XHDPE}+2\right)\left(1-\left(1-\zeta_{XHDPE}\right)^{1/2}\right)^{2}} \quad (2)$$

where ν_{XHDPE} and ν_{DXHDPE} are, respectively, the crosslink density of XHDPE and decrosslinked XHDPE, ζ_{XHDPE} and ζ_{DXHDPE} are, respectively, the gel fraction of XHDPE and decrosslinked XHDPE, M_n is the number average molecular weight of the uncrosslinked HDPE. Since the value of M_n is not available, the weight average molecular weight, M_w, of HDPE is used in calculation of Eq. (2). The M_w of HDPE is 5.2×10^4 g/mole [15]. Eq. (1) is used to describe the relationship between the normalized gel fraction and the normalized crosslink density of decrosslinked XHDPE in the case when only the breakage of main chains occurs. Eq. (2) is used in case when only crosslinks are broken. Therefore, the type of preferential bond breakage during decrosslinking of XHDPE can be identified by using Horikx functions. Figure 4 shows the normalized gel fraction versus the normalized crosslink density of decrosslinked 1% (a), 2% (b) and 4% (c) XHDPE. The normalized gel fraction and crosslink density of decrosslinked XHDPE are defined with respect to the values of XHDPE. The dotted and dashed lines in Figure 4 are

drawn for cases when only the breakage of main chains and crosslinks occur according to Eqs. (1) and (2), respectively. It is seen from Figure 4 that all decrosslinked XHDPEs obtained from the same XHDPE at different processing conditions indicates a similar type of bond breakage. It can be inferred that the gel fraction and crosslink density of XHDPE is a dominating factor in the type of bond breakage during decrosslinking of XHDPE. Also, it is seen from Figure 4 that a separation of curves related to the main chain breakage (curve 1) and crosslink breakage (curve 2) increases with the degree of crosslinking. This indicates that the gel fraction of decrosslinked XHDPE becomes more sensitive to the type of preferential bond breakage when the degree of crosslinking of XHDPE increases. It is seen from Figure 4a that the data for decrosslinked 1 % XHDPE lie below the main chain breakage curve. This indicates that the main chain breakage is due to both the thermal and mechanical degradation. At the same time it is seen from Figures 4b and 4c that the results for decrosslinked 2% and 4% XHDPE lie between the main chain breakage and crosslink breakage curves and more close to the crosslink breakage curve. It is very likely that more breakage of crosslinks than main chains takes place during decrosslinking of 2% and 4% XHDPE. Obviously, decrosslinking of 2% and 4% XHDPE exhibits a higher preference to the breakage of crosslinks than that of 1% XHDPE. Since the data for decrosslinked 2% XHDPE is more close to the corresponding crosslink breakage curve than the data for decrosslinked 4% XHDPE, it is very likely that decrosslinking of 2% XHDPE exhibits a higher preference of the breakage of crosslinks than decrosslinking of 4% XHDPE. Besides, the difference in the barrel pressure may also affect the type of preferential bond breakage during decrosslinking of 4% XHDPE. More breakage of main chains during decrosslinking of 4% XHDPE occurs when the barrel pressure is higher, as seen from Figure 4c.

In order to discuss the effect of the degree of crosslinking on decrosslinking of XHDPE, the decrease of the crosslink density rather than the decrease of the gel fraction is chosen as the measure of this effect. Decrosslinking of XHDPE is a process of cleavage of the main chain and crosslink. To characterize decrosslinking one needs to specify the number of the broken bonds. Neglecting the radical initiated chemical reaction and assuming the crosslink network in XHDPE is an ideal tetrafunctional crosslink network, a relationship between the decrease of the crosslink density and the number of the broken main chains and crosslinks per unit volume becomes:

$$\Delta \nu = \nu_{XHDPE} - \nu_{DXHDPE} = n_{mc} + 2n_{xl} \quad (3)$$

where $\Delta\nu$ is the decrease of the crosslink density, n_{mc} and n_{xl} are the number of broken main chains and crosslinks per unit volume, respectively. The maximum and minimum values of $\Delta\nu$ of decrosslinked 1%, 2% and 4% XHDPE are tabulated in Table 1. As shown in Table 1, the maximum and minimum values of $\Delta\nu$ of decrosslinked XHDPE increase with the degree of crosslinking of XHDPE. The value of $\Delta\nu$ of decrosslinked 4% XHDPE is about 4 times of that of decrosslinked 2% XHDPE. Therefore, according to Eq. (3), the number of the broken bonds per unit volume during decrosslinking of 4% XHDPE is higher than that during decrosslinking of 2% XHDPE, regardless of the type of bond broken. Similarly, the number of the broken chemical bonds per unit volume during decrosslinking of 2% XHDPE is higher than that during decrosslinking of 1% XHDPE. Thus, it can be concluded that the number of broken chemical bonds increases with the degree of crosslinking of XHDPE. In other word, a more intensive rupture of the crosslink network happens in XHDPE of the higher crosslink density.

Dynamic Properties

Figures 5 to 8 shows, respectively, the frequency dependences of the storage modulus, loss modulus, complex viscosity and loss tangent of decrosslinked 1% (a), 2% (b) and 4% (c) XHDPE obtained without and with ultrasonic treatment at various amplitudes at a temperature of 160^{o}C. The frequency dependences of the dynamic properties of XHDPE are also indicated in Figures 5 to 8. It is seen from Figures 5 to 7 that the storage and loss moduli and complex viscosity of XHDPE and decrosslinked XHDPE exhibit almost a power law dependence on the frequency. Also, the loss tangent of XHDPE and decrosslinked XHDPE exhibits weak frequency dependence. Such dynamic rheological behavior is similar to a typical behavior of so-called "critical gel" [21-27] and "post critical gel" [21, 28] within the frequency range below the rubbery plateau. The storage modulus of XHDPE and decrosslinked XHDPE is below the plateau modulus of HDPE. Thus, the dynamic rheological behavior of the XHDPE and decrosslinked XHDPE can be considered as the typical behavior of the critical gel and post critical gel.

It is seen from Figures 5 to 8 that the storage modulus and complex viscosity of XHDPE increase with the degree of crosslinking of XHDPE, whereas the loss modulus and loss tangent decrease with the degree of crosslinking of XHDPE. The frequency dependence of the storage modulus of XHDPE becomes weaker as the degree of crosslinking of XHDPE increases. For 4% XHDPE, its storage modulus is virtually independent of the frequency. These phenomena are clearly due to the fact that XHDPE of the higher degree of crosslinking is comprised of a more rigid crosslink network of a higher elasticity. Also, it is seen from Figures 5, 7 and 8 that decrosslinked XHDPE exhibits a lower storage modulus and complex viscosity and a higher loss tangent than those of XHDPE with the effect being larger at higher ultrasonic amplitudes. The loss modulus of decrosslinked XHDPE decreases with the ultrasonic amplitude, as seen from Figure 6. It is seen that there are crossovers between the loss modulus of XHDPE and decrosslinked XHDPE obtained at some processing conditions. The decrosslinked XHDPE consists of gel and sol. Relaxation of the gel occurs due to the presence of the dangling chains. Relaxation of the sol is the process which is typical for uncrosslinked polymers. Thus, the difference in the relaxation time of the dangling chains in the network and the polymer chains in the sol may lead to such a crossover.

The study on decrosslinking of 1% XHDPEs obtained at different processing conditions [15] indicates that their dynamic properties can be well correlated with the gel fraction and crosslink density. However, such a relationship between the dynamic properties of 2 and 4 % decrosslinked XHDPE and their gel fraction and crosslink density is invalid. For example, as seen from a comparison of Figures 5 to 8 with Figure 3, the storage and loss moduli and complex viscosity of decrosslinked XHDPE obtained from XHDPE of different degrees of crosslinking at the same processing conditions does not correlate with the gel fraction and crosslink density of decrosslinked XHDPE. Only the loss tangent of decrosslinked XHDPE obtained from XHDPE of different degrees of crosslinking at the same processing conditions correlates with these quantities. Namely, it decreases with an increase of the gel fraction and crosslink density. However, the previous study [15] indicated the existence of correlation of the storage modulus, complex viscosity and loss tangent of decrosslinked XHDPE with the gel fraction and crosslink density. To understand this phenomenon, it is important to note that decrosslinked XHDPE is comprised of the gel and sol. In fact, the decrosslinked XHDPE of the present study contains at least 29% sol fraction (see Figure 3). This indicates that the dynamic properties of decrosslinked

XHDPE is not only related to its gel fraction and crosslink density but also influenced by the molecular structure of its sol. As will be shown later, the lower storage and loss moduli and complex viscosity of decrosslinked 2% and 4% XHDPEs are caused by the lower molecular weight of the sol.

As mentioned earlier, the molecular structure of sol of decrosslinked XHDPE not only influences the dynamic properties of decrosslinked XHDPE, but also provides information about the type of bonds broken during decrosslinking of XHDPE. It should be noted that the sol of decrosslinked XHDPE is not only generated by the decrosslinking process but also inherently present in XHDPE. For example, the 1% XHDPE contains 19.5 wt% of sol. By neglecting possible radical initiated reaction during decrosslinking of XHDPE, one can find that in decrosslinked 1% XHDPE without ultrasonic treatment 59 wt% of the sol is generated by decrosslinking and 41 wt% of the sol is inherited. It is impossible to physically separate the generated and inherited sols of decrosslinked XHDPE. To reduce the effect of the inherited sol, the decrosslinked XHDPE obtained at an amplitude of 10 μm is selected for further discussion. The amount of generated and inherited sols of decrosslinked XHDPE obtained with the die at an amplitude of 10 μm are, respectively, 64.5 wt% and 35.5 wt% for decrosslinked 1% XHDPE, 86.4 wt% and 13.6 wt% for decrosslinked 2% XHDPE and 97.5 wt% and 2.5 wt% for decrosslinked 4% XHDPE. By doing so, the influence of the inherited sol on dynamic properties of the total sol of decrosslinked XHDPE is minimized, especially for the case of decrosslinked 2% and 4% XHDPE.

Figure 9 shows the frequency dependence of the complex viscosity of the HDPE (a), sol of 1% XHDPE (b), sol of decrosslinked 1% (c) and 2% (d) XHDPE obtained with the die, and sol of decrosslinked 4% XHDPE obtained without (e) and with (f) the die at an amplitude of 9 μm at temperatures of 140, 150 and 160^{o}C. Cross model [29] fits are also indicated in Figure 9. The following two equations are used for this fitting:

$$|\eta^*| = \frac{\eta_o^*(T)}{1+\left[\frac{\eta_o^*(T)\omega}{\tau}\right]^{1-n}} \quad (4)$$

$$\eta_o^*(T) = A\exp(\frac{T_b}{T}) = A\exp(\frac{E}{RT}) \quad (5)$$

where, A, T_b, τ and n are fitting parameters. The function of $\eta_o^*(T)$ is the temperature dependency of the zero-frequency viscosity by the Arrhenius equation where T is the temperature, E is the activation energy for flow and R is the gas constant.

It is seen from Figure 9 that HDPE exhibits a typical terminal behavior with a Newtonian viscosity region, whereas sols of 1% XHDPE and decrosslinked XHDPE exhibit a strong non-Newtonian behavior. The viscosity of the sol of 1% XHDPE is lower than that of HDPE. This is due to the fact that the low molecular fraction of HDPE has a lower probability to be incorporated into the crosslink network during crosslinking of HDPE. The viscosity of the sol of decrosslinked XHDPE decreases with the degree of crosslinking of XHDPE and a substantial difference (about one order of the magnitude) is seen from Figure 9c to 9f. This indicates that the molecular weight of the sol of decrosslinked XHDPE decreases with the degree of crosslinking of XHDPE. This observation can be correlated with the number of broken chemical bonds per unit volume in decrosslinked XHDPE which is shown to significantly increase with the degree of crosslinking of XHDPE. Since the generated sol of decrosslinked XHDPE is produced by the cleavage of the main chains and crosslinks of XHDPE, the sol of a lower molecular weight is obtained from decrosslinking process of XHDPE with the number of broken chemical bonds per unit volume being significantly higher. The decrease of the complex viscosity of sol with the degree of crosslinking of XHDPE also explains why the complex viscosity of decrosslinked XHDPE does not correlate with the gel fraction and crosslink density. It is due to the fact that the decrosslinked XHDPE also contains the sol whose molecular weight decreases with the degree of crosslinking, though the gel fraction and crosslink density of decrosslinked XHDPE increases with the degree of crosslinking of XHDPE.

The presence of branching in polymers can be detected by comparing the activation energy for flow of linear and branched polymers. It is seen from Table 2 that the activation energy of HDPE and the sol of 1% XHDPE are, respectively, lowest and highest among all the studied samples. Since HDPE is a linear polymer, it has the lowest activation energy. The peroxide initiated crosslinking of HDPE is a radical reaction with the interlink reaction between

the HDPE molecules occurring before the gel formation. Accordingly, the branched structure is certainly created during the interlink reaction, as evidenced by a high value of the activation energy of the sol of 1% XHDPE. It is possible that the interlink reaction may occur between the two chains whose radicals at the chain ends. However, since the interlink reaction is a statistical random process, the possibility of two chains whose radicals at the chain ends combine together is very low. Thus, the branched structure of the sol of 1% XHDPE is a result of the interlink reaction. It is also seen from Table 2 that the activation energy of the sol of decrosslinked 1% XHDPE is very close to that of the sol of 1% XHDPE. As mentioned earlier, 64.5 wt% of the sol is generated. The activation energy of this sol is close to that of the sol of 1% XHDPE. Thus, the activation energy of the sol generated during decrosslinking of 1% XHDPE can be approximated as that of the total sol of decrosslinked 1% XHDPE. Furthermore, the activation energy of the sol of decrosslinked 4% XHDPE is lower than that of the sol of decrosslinked 2% XHDPE which in turn is lower than that of decrosslinked 1% XHDPE. Clearly, the activation energy of the sol of decrosslinked XHDPE decreases with the degree of crosslinking of XHDPE. In particular, the activation energy of PE is solely dictated by its branched structure as long as its molecular weight is higher than the critical molecular weight [30]. It is usually considered that a higher activation energy for flow corresponds to a more branched structure [31-36]. Crosslinks in the peroxide crosslinked XHDPE are carbon-carbon bonds and their breakage alone should not generate branches during decrosslinking of XHDPE. Only the breakage of main chains would generate branches. According to the above analysis, the preferential breakage of crosslinks increases with the degree of crosslinking of XHDPE. This conclusion seems to contradict with the observation made from the analysis based on the Horikx function. However, it should be pointed out that the activation energy for flow is not only influenced by the number and length of branches [31-36]. The activation energy of PE significantly increases with the molecular weight of branches in case when its molecular weight is higher than the molecular weight between entanglement (M_e). The exact topology of the sol of decrosslinked XHDPE is difficult to determine in the presence of the multi-level branched structure generated during decrosslinking of XHDPE. The length of branches can be approximated by assuming that the breakage of main chains takes place at the middle of polymer chains. The average molecular weight between crosslinks (M_c) in XHDPE is defined as

$$M_c = \frac{\rho}{\nu} \quad (6)$$

where ρ is the density and ν is the crosslink density of XHDPE. According to Eq. 6, the M_c of the 1%, 2% and 4% XHDPE are, respectively, 5.4×10^4, 6.7×10^3, 1.9×10^3 g/mole. Thus, if one neglects the presence of the multi-level branched structure, the average molecular weight of chain branches in the sol of decrosslinked 1%, 2% and 4% XHDPE is, respectively, 2.7×10^4, 3.4×10^3, 9.5×10^2 g/mole. The value of M_e for PE is about 1.0×10^3 g/mole [35, 37]. Consequently, the chain branches in the sol of decrosslinked 4% XHDPE are not well-entangled, while they are entangled in the sol of decrosslinked 1% and 2% XHDPE. This leads to a higher activation energy of the sol of decrosslinked 2% XHDPE than that of the sol of decrosslinked 4% XHDPE.

The effect of the barrel pressure on the type of preferential bond breakage during decrosslinking of 4% XHDPE is also revealed through a comparison of the activation energy of the sol of decrosslinked 4% XHDPE without and with the die. As seen from Table 2, the former exhibits a lower activation energy than the latter indicating a more breakage of crosslinks in the case of lower barrel pressure. This is in agreement with the analysis of Horikx function (see Figure 4c).

FTIR study

Figure 10 shows the FTIR spectra of the 1%, 2% and 4% XHDPE (a) and decrosslinked 1%, 2% and 4% XHDPE obtained at an amplitude of 10 μm from SSE with die (b). These three decrosslinked XHDPE samples are selected because the changes of their molecular structure are most significant among the decrosslinked XHDPE. Identification of the peaks in FTIR spectra is based on IR Library. The strong absorption peaks at 2850 cm^{-1} and 2914 cm^{-1} correspond to the CH_2 symmetrical and asymmetrical stretching mode, respectively. The peak at 1462 cm^{-1} corresponds to the C-H bending mode. Also, a weak peak at 730 cm^{-1} corresponds to the rocking deformation of CH_2. These peaks indicate that the XHDPE and decrosslinked XHDPE exhibits a typical chemical structure of PE. During decrosslinking of the XHDPE, the radicals can be generated as a result of the breakage of the main chains and crosslinks. Thus, in the presence of oxygen, it is possible that the thermooxidative degradation of the decrosslinked XHDPE may

occur. As seen from Figure 10, no absorption peak corresponding to thermooxidative species including ester group (1743 cm^{-1}), aldehyde (1733 cm^{-1}), ketone (1720 cm^{-1}) and acid (1712 cm^{-1}) groups [28] is seen on the FITR spectra of the decrosslinked 1%, 2% and 4% XHDPE. Also, there is no new peak present in the FTIR spectra of the decrosslinked XHDPE in comparison with that of the XHDPE. Thus, it is concluded that there is no evidence of appreciable thermooxidative degradation of the decrosslinked XHDPE. This is due to the fact that the decrosslinking of XHDPE occurs in the fully filled region of the extruder where the oxygen concentration is insignificant. However, one can see the presence of a weak peak at 875 cm^{-1} for all the samples in Figure 10. This peak is the characteristic peak of calcium carbonate which is the carrier of dicumyl peroxide.

DSC Analysis

Figure 11 shows melting temperature (a) and crystallinity (b) of decrosslinked XHDPE as a function of the ultrasonic amplitude. The values for HDPE and XHDPE are also indicated. As seen from Figure 11, the melting temperature and crystallinity of XHDPE is lower than those of HDPE and decreases with the degree of crosslinking. This is due to the presence of crosslinks in the gel and the branched structure in the sol of XHDPE hindering the formation of the PE crystal [37]. It is also seen from Figure 11 that the melting temperature and crystallinity of decrosslinked 2% and 4% XHDPE are higher than those of the corresponding XHDPE. This is the result of a significant decrease of the crosslink density during decrosslinking of 2% and 4% XHDPE. Meanwhile, the crystallinity and melting temperature of decrosslinked 1% XHDPE are, respectively, higher and slightly lower than those of 1% XHDPE. The increase of the crystallinity of decrosslinked 1% XHDPE is clearly the result of a reduction of the crosslink density and gel fraction. However, a slight decrease of the melting temperature of decrosslinked 1% XHDPE is likely due to the presence of high molecular weight chain branches hindering the growth of the lamellar structure.

Figure 11 also shows that the melting temperature and crystallinity of decrosslinked XHDPE exhibits different trend with the ultrasonic amplitude. The previous study [15] on decrosslinking of 1% XHDPE revealed that the crystallinity and melting temperature does not always increase with the amplitude, even though the gel fraction and crosslink density decrease

substantially. It is due to the fact that the melting temperature and crystallinity of decrosslinked XHDPE are affected by the gel fraction and crosslink density of decrosslinked XHDPE and the molecular structure in its sol. The decrease of the gel fraction and crosslink density certainly increases the melting temperature and crystallinity. This is a natural result of the reduced hindrance during the growth of the PE lamellar structure. However, the presence of branched structure in the sol also decreases the melting temperature and crystallinity of decrosslinked XHDPE. Thus, the melting temperature and crystallinity of decrosslinked XHDPE are dependent on these two competing effects and, therefore, significantly influenced by the type of bond breakage during decrosslinking of XHDPE. The melting temperature and crystallinity of decrosslinked 2% XHDPE show a slight decrease at an amplitude of 5 μm but exhibits a significant increase at amplitudes of 7.5 and 10 μm. This trend is reverse to that of the gel fraction and crosslink density of decrosslinked 2% XHDPE on the amplitude (Figure 3) indicating a higher preference to the breakage of crosslinks during decrosslinking of 2% XHDPE. In contrast, decrosslinking of 1% and 4% XHDPE exhibits a lower preference to the breakage of crosslinks than decrosslinking of 2% XHDPE. Hence, the melting temperature and crystallinity of the ultrasonically decrosslinked 1% and 4% XHDPE show no correlation with the ultrasonic amplitude.

The effect of the different type of preferential bond breakage can be further elaborated by comparing the melting temperature and crystallinity of decrosslinked XHDPE obtained at the same processing conditions on XHDPE of different degree of crosslinking. For instance, the gel fraction and crosslink density of decrosslinked 2% XHDPE obtained at amplitudes of 7.5 and 10 μm are higher than those of decrosslinked 1% XHDPE at same amplitudes. However, the melting temperature and crystallinity of decrosslinked 2% XHDPE are virtually same as those of decrosslinked 1% XHDPE. This is attributed to a higher preference to the breakage of crosslinks during decrosslinking of 2% XHDPE than decrosslinking of 1% XHDPE. Also, the melting temperature and crystallinity of decrosslinked 4% XHDPE obtained at an amplitude of 10 μm without the die are virtually same as those with the die. Although the gel fraction of former is higher than that of latter and the sol of the former is less branched than that of the latter, as indicated by the activation energy.

Tensile Properties

Figure 12 shows the stress-strain curves of XHDPE, decrosslinked 1% and 2% XHDPE with the die and decrosslinked 4% XHDPE without the die at an amplitude of 10 μm. The stress-strain behavior of decrosslinked XHDPEs without and with the ultrasonic treatment at other amplitudes and decrosslinked 4% XHDPE with the die at amplitude of 10 μm exhibits similar features, as indicated in Figure 12. It is seen from Figure 12 that an increase of the degree of crosslinking of XHDPE leads to a decrease of the yield stress, strain at break and stress at break. Decrosslinked 1% and 2% XHDPE yields ductile materials with a well-developed necking plateau at intermediate strains and strain hardening behavior at high strains, whereas decrosslinked 4% XHDPE yields a brittle material without necking and strain hardening. The slope of stress-strain curves of decrosslinked 1% and 2% XHDPE in the strain hardening region is lower than that of the corresponding XHDPE.

Figure 13 shows the Young's modulus (a), yield stress (b), strain at break (c) and stress at break (d) of various decrosslinked XHDPE as a function of the ultrasonic amplitude. The values for HDPE and XHDPE are also indicated in Figure 13. HDPE exhibits the highest Young's modulus of 1.4 GPa among all the studied samples due to its high crystallinity. The Young's modulus of XHDPE decreases with the degree of crosslinking, as a result of a decrease of the crystallinity. As seen from Figure 13a, decrosslinked 1% and 2% XHDPE exhibits a higher Young's modulus than XHDPE, as a result of an increase of the crystallinity caused by decrosslinking. An increase of the ultrasonic amplitude does not significantly increase the Young's modulus of decrosslinked 1% and 2% XHDPE, except for decrosslinked 1% XHDPE obtained at an amplitude of 10 μm which exhibits a higher Young's modulus. The previous study [15] revealed that the Young's modulus increases with a decrease of the gel fraction and crosslink density of decrosslinked 1% XHDPE due to a change of its lamellar morphology. Thus, the increase of the Young's modulus of decrosslinked 1% XHDPE obtained at an amplitude of 10 μm is due to a significant decrease of the gel fraction and crosslink density [15]. It is also seen from Figure 13a that decrosslinked 4% XHDPE obtained at an amplitude of 5 μm exhibits a lower Young's modulus than that of 4% XHDPE. As previously shown [15], decrosslinked XHDPE consists of gel particles and sol matrix. Since the polymer chains in the gel particle are less mobile, they cannot entangle with the polymer chains in other gel particles. Therefore, the load transfer between the gel particles relies on the polymer chains in the sol matrix. Since the molecular weight of the sol of decrosslinked 4% XHDPE is low, it cannot effectively bridge the

gel particles when the gel fraction is high. Hence, the Young's modulus of decrosslinked 4% XHDPE obtained at an amplitude of 5 μm exhibits a lower Young's modulus than that of 4% XHDPE. An increase of the amplitude leads to a substantial increase of the Young's modulus of decrosslinked 4% XHDPE, as a result of a decrease of the gel fraction.

As shown in Figure 13b, among all the samples HDPE exhibits the highest yield stress due to its high crystallinity. The yield stress of XHDPE decreases with the degree of crosslinking as a result of a decrease of the crystallinity. It is also seen from Figure 13b that decrosslinked XHDPE exhibits a higher yield stress than the corresponding XHDPE due to an increase of the crystallinity. The increase of the amplitude does not change the yield stress of decrosslinked XHDPE significantly, even though there is an increase of the crystallinity of decrosslinked 2% XHDPE with the amplitude. It is known that the yield stress of PE is not solely dependent on its crystallinity. In fact, the structure-yield stress relationship of PE is still an unresolved issue [38-42]. Two competing models, namely, the screw dislocation model [43] and the mechanical melting model [44], are used to describe the tensile yielding of PE. The former considers the yield stress is a function of the lamella thickness and the latter considers that it is a function of the crystallinity. Both the models are supported by extensive experimental studies but none can successfully describe the structure-yield stress relationship of PE of various molecular structures within a unified framework [38-42]. It seems that these models cannot provide a satisfactory description on this relationship for PE having a complex molecular structure. The study [42] tried to reconcile these two competing models with some success. In our opinion, the structure-yield relationship of PE is very complicated due to the fact that the semicrystalline morphology of PE is sensitive to its molecular structure. Therefore, an insignificant effect of processing conditions on the yield stress of decrosslinked XHDPE is caused by its complex molecular structure. It should be noted that decrosslinked 4% XHDPE without and with the ultrasonic treatment at an amplitude of 5 μm breaks even before it reaches yielding.

Among all the samples, as seen from Figure 13c, the strain at break of virgin HDPE is highest due to its linear molecular structure. The strain at break of XHDPE decreases with the degree of crosslinking as a result of an increase of the gel fraction and crosslink density. It is due to the fact that the presence of crosslinks hinders the slippage of chains during the deformation. It is also seen from Figure 13c that the strain at break of decrosslinked 1% and 2% XHDPE are,

respectively, lower and higher than that of the corresponding XHDPE. The difference in the effect of decrosslinking of 1% and 2% XHDPE on the strain at break is caused by the different preference to the type of broken bonds during decrosslinking. Due to the occurrence of the preferential breakage of crosslinks during decrosslinking of 2% XHDPE, decrosslinking can be viewed as the reverse reaction to crosslinking of HDPE. Since the strain at break of XHDPE decreases with the gel fraction and crosslink density, decrosslinking of 2% XHDPE leads to an increase of the strain at break of decrosslinked 2% XHDPE, due to a decrease of the gel fraction and crosslink density with the amplitude. However, a slight decrease of the strain at break of decrosslinked 2% XHDPE obtained at an amplitude of 10 μm, as seen in Figure 13c, is attributed to an increase of the branched sol. The strain at break of decrosslinked 1% XHDPE is lower than that of 1% XHDPE. This is due to the fact that a less preferential breakage of crosslinks occurs during decrosslinking of 1% XHDPE. An increase of the amplitude insignificantly affects the strain at break of decrosslinked 1% XHDPE. The latter is due to two competing effects on the strain at break of decrosslinked 1% XHDPE. Specifically, a decrease of the gel fraction and crosslink density leads to a higher mobility of chains increasing the strain at break of decrosslinked 1% XHDPE. However, the branched structure of the sol of decrosslinked 1% XHDPE generated during its decrosslinking decreases the strain at break. Thus, no significant differences in the strain at break of decrosslinked 1% XHDPE obtained at different amplitudes are observed. The strain at break of decrosslinked 4% XHDPE containing a sol of the low molecular weight is lower than that of 4% XHDPE. The strain at break of decrosslinked 4% XHDPE increases with the amplitude, as a result of a decrease of the gel fraction.

The stress at break of ductile PE is determined by the strain at break and the slope of strain-stress curve at high strains. As shown in Figure 13d, the stress at break of XHDPE decreases with the degree of crosslinking, as a result of a decrease of the strain at break with the degree of crosslinking. The stress at break of HDPE is lower than that of 1% XHDPE but higher than that of 2% XHDPE. This is due to a high strain at break and a low slope of the strain-stress curve at high strains. The stress at break of decrosslinked 2% XHDPE, due to its higher strain at break, is higher than that of 2% XHDPE. The stress at break of decrosslinked 2% XHDPE is insignificantly affected by the amplitude, since an increase of the amplitude leads to an increase of the strain at break and to a decrease of the slope of stress-strain curves at high strains. Due to these two competing effects, the stress at break of decrosslinked 2% XHDPE is insignificantly

affected by the ultrasonic amplitude. Similarly, the lower stress at break of decrosslinked 1% XHDPE than that of 1% XHDPE is due to a similar consideration. It is seen in Figure 13d that the stress at break of decrosslinked 4% XHDPE without the die is higher than that of 4% XHDPE. This is because this sample breaks before reaching the necking plateau. The stress at break of decrosslinked 4% XHDPE obtained with the die at an amplitude of 10 μm is lower than that of 4% XHDPE. Due to the presence of the sol of a low molecular weight in decrosslinked 4% XHDPE with die at an amplitude of 10 μm, its breakage occurs at necking plateau region without exhibing a strain-hardening behavior. Since 4% XHDPE exhibits a strain-hardening behavior, its stress at break is higher than that of decrosslinked 4% XHDPE obtained with die at an amplitude of 10 μm.

Conclusions

Extrusion of XHDPE of various degrees of crosslinking is performed by means of an ultrasonic SSE without and with ultrasonic treatment. The barrel pressure and ultrasonic power consumption are recorded during the extrusion. Swelling test, SAOS, thermal analysis and tensile test are employed to determine the gel fraction, crosslink density, dynamic properties, melting temperature, crystallinity and tensile properties of HDPE, XHDPE and decrosslinked XHDPE.

The barrel pressure decreases and ultrasonic power consumption increases with the amplitude. The barrel pressure increases with the degree of crosslinking of XHDPE. The ultrasonic power consumption is insignificantly affected by the degree of crosslinking of XHDPE and increases with the barrel pressure.

The mechanical shear during the extrusion of XHDPE leads to a substantial decrease of the gel fraction and crosslink density of decrosslinked XHDPE. The ultrasonic treatment further decreases the gel fraction and crosslink density of decrosslinked XHDPE. The analysis based on the Horikx function indicates type of the preferential bond breakage which is significantly affected by the degree of crosslinking of XHDPE. Also, it is found that a more intensive rupture of the crosslink network occurs in XHDPE of higher degree of crosslinking. In particular, the crosslink density of the decrosslinked 1%, 2% and 4% XHDPE obtained at an amplitude of 10 μm is, respectively, reduced by 69%, 94% and 98% in comparison to that of XHDPE. This

decrosslinking occurs without appreciable thermooxidative degradation as indicated by the FTIR spectra.

The dynamic properties of XHDPE and decrosslinked XHDPE are not only affected by the gel fraction and crosslink density but also by the molecular structure of the sol. The activation energy of various sols of decrosslinked XHDPE indicates the type of preferential bond breakage during decrosslinking of XHDPE of various degree of crosslinking. The melting temperature, crystallinity and tensile properties of decrosslinked XHDPE is significantly affected by the type of preferential bond breakage during decrosslinking of XHDPE. The tensile properties of the decrosslinked 2% XHDPE are superior to those of the 2% XHDPE and to the best of our knowledge, not reported in earlier studies.

It is interesting to point out that most studies on the type of preferential bond breakage during decrosslinking of crosslinked polymers and devulcanization of rubbers are related to the bond energy. Since the chemical bonds in the main chains and crosslinks in XHDPE are same, the difference in the type of preferential bond breakage during decrosslinking of XHDPE of different degree of crosslinking cannot be explained by the bond energy alone. Instead, the preferential bond breakage seems to be a function of the structural characteristics of the crosslink network. Considering the importance of the type of preferential bond breakage in decrosslinking of crosslinked polymers and devulcanization of rubber vulcanizates, more efforts needed to be directed toward further understanding of the relationship between the type of preferential bond breakage and structure of the network.

Acknowledgements

Financial support for this work by NSF grant No. CMMI-1131342 is greatly appreciated. Authors wish to thank the Exxon Mobil Chemical Company for providing HDPE and the Akrochem Corporation for providing peroxide and antioxidant.

References

1. T. Goto, T. Yamazaki, T. Sugeta, I. Okajima, T. Sako, Selective decomposition of the siloxane bond constituting the crosslinking element of silane-crosslinked polyethylene by supercritical alcohol, *J. Appl. Polym. Sci*., 109, 144(2008).
2. H.-S. Lee, J. H. Jeong, G. Hong, H.-K. Cho, B. K. Baek, C. M. Koo, S. M. Hong, J. Kim, Y. W. Lee, Effect of solvents on decrosslinking of crosslinked polyethylene under subcritical and supercritical conditions, *I & EC Research*., 52, 6633 (2013).
3. H. Lee, J.H. Jeong, H.K. Cho, C.M. Koo, S.M. Hong, H. Kim, Y.W. Lee, A kinetic study of the decrosslinking of crosslinked polyethylene in supercritical methanol, *Polym. Degrad. Stability*, 93, 2084(2008).
4. X. Zhang, C. Lu, M. Liang, Preparation of thermoplastic vulcanizates on waste crosslinked polyethylene and ground tire rubber through dynamic vulcanization, *J. Appl. Polym. Sci*., 122, 2110(2011).
5. H. Wu, M. Liang, C. Lu, Morphological and structural development of recycled crosslinked polyethylene during solid-state mechanochemical milling, *J. Appl. Polym. Sci*., 122, 257(2011).
6. S.S. Oh, D.S. Bang, J.K. Lee, Recycling of waste XLPE using a modular intermeshing co-rotating twin screw extruder, *Elastomer*, 39, 131(2004).
7. C.C. White, J. Wagenblast, M.T. Shaw, Separation, size reduction, and processing of XLPE from electrical transmission and distribution cable, Polym. Eng. Sci., 40, 863(2000).
8. A.I. Isayev, S. Ghose, Ultrasonic Devulcanization of Used Tires and Waste Rubbers, in book Rubber Recycling, Eds. De SK, Isayev AI, Khait K. CRC Press, Boca Raton, Chapter 9, pp. 311-384, 2005.
9. A.I. Isayev, Recycling of Rubber, in book Science and Technology of Rubber, Eds. Mark JE, Erman B., Eirich FR. 3rd Ed., Academic Press, New York, Chapter 15, pp. 663-701, 2005.
10. C. K. Hong, A.I. Isayev, Ultrasonic devulcanization of unfilled SBR under static and continuous conditions, *Rubber Chem. Technol*., 75, 133 (2002).
11. S. Yushanov, A.I. Isayev, V.Y. Levin, Percolation simulation of the network degradation during ultrasonic devulcanization, *J. Polym. Sci. B Polym. Phys* 34, 2409 (1996).

12. X. Sun, A.I. Isayev, Ultrasound devulcanization: comparison of synthetic isoprene and natural rubbers, *J. Mat. Sci*., 17, 7520 (2007).
13. V. V. Yashin, A.I. Isayev, A Model for rubber degradation under ultrasonic treatment: part II. rupture of rubber network and comparison with experiments, *Rubber Chem. Technol.*, 73, 325 (2000).
14. A.I. Isayev, J. Jenkins, Ultrasonic decrosslinking of crosslinked polyethylene, *SPE ANTEC Technical Papers*, 53, 109 (2008).
15. A.I. Isayev, K. Huang, Decrosslinking of crosslinked high-density polyethylene via ultrasonically aided single-screw extrusion. *Poly. Eng. Sci.* doi: 10.1002/pen.23827
16. P.J. Flory, Statistical mechanics of swelling of network structures, *J. Chem. Phys.*, 18, 108 (1950).
17. T.S.K. Ng, and G.H. McKinley, Power law gels at finite strains: The nonlinear rheology of gluten gels, *J. Rheol*. 52, 417 (2008).
18. L. Zhu, F. Chiu, Q. Fu, R.P. Quirk, S.Z.D. Cheng, in book Polymer Handbook, 4th Ed., John Wiley & Sons, pp V-17, 1999.
19. C.K. Hong, A.I. Isayev, An application of high-power ultrasound to rubber recycling, *Elastomer*, 38, 103 (2003).
20. V.V. Yashin, A.I. Isayev, A model for rubber degradation under ultrasonic treatment: Part I. acoustic cavitation in viscoelastic solid, *Rubber Chem. Technol.*, 72, 741 (1999).
21. M.E. De Rosa, H.H. Winter, The effect of entanglements on the rheological behavior of polybutadiene critical gels, *Rheol. Acta*., 33, 220 (1994).
22. M.M. Horikx, Chain scissions in a polymer network, *J. Polym. Sci*., 19, 445 (1956).
23. H.H. Winter, F. Chambon, Analysis of linear viscoelasticity of a crosslinking polymer at the gel point, *J. Rheol.*, 30, 367 (1986).
24. F. Chambon, H.H. Winter, Linear viscoelasticity at the gel point of a crosslinking PDMS with imbalanced stoichiometry, *J. Rheol.*, 31, 683 (1987).
25. E.M. Vallés, J.M. Carella, H.H. Winter, M. Baumgaertel, Gelation of a radiation crosslinked model polyethylene, *Rheol. Acta*, 29,535 (1990).
26. M. Yamaguchi, K.-I. Suzuki, S. Maeda, Enhanced strain hardening in elongational viscosity for HDPE/crosslinked HDPE blend. I.Characteristics of crosslinked HDPE, *J. Appl. Polym. Sci.*, 86, 73 (2002).

27. X. Zhang, H. Yang, Y. Song, Q. Zheng, Rheological behaviors of randomly crosslinked low density polyethylene and its gel network, *Polymer*, 53, 3035 (2012).
28. V.H. Rolón-Garrido, M.H. Wagner, Elongational rheology and cohesive fracture of photo-oxidated LDPE, *J. Rheol*., 58, 199 (2014).
29. M.M. Cross, Relation between viscoelasticity and shear-thinning behavior in liquids, *Rheol. Acta.*, 18, 609 (1979).
30. D. Pearson, G. Ver Strate, E.D. Von Meerwall, F. Schilling, Viscosity and self-diffusion coefficient of linear polyethylene, *Macromol.*, 20, 1133 (1987).
31. H. Mavridis, R. Shroff, Temperature dependence of polyolefin melt rheology, *Poly. Eng. Sci.*, 32, 1778 (1992).
32. D. Lohse, S. Milner, L. Fetters, M. Xenidou, N. Hadjichristidis, R. Mendelson, C. Garcia-Franco, M. Lyon, Well-Defined, Model Long Chain Branched Polyethylene. 2. Melt Rheological Behavior, *Macromol.*, 35, 3066 (2002).
33. V. Raju, G. Smith, G. Marin, J. Knox, W. Graessley, Properties of amorphous and crystallizable hydrocarbon polymers. I. Melt rheology of fractions of linear polyethylene, *J. Polym. Sci. B Polym. Phys.*, 17, 1183 (1979).
34. W. Rochefort, G. Smith, H. Rachapudy, V. Raju, W. Graessley, Properties of amorphous and crystallizable hydrocarbon polymers. II. Rheology of linear and star-branched polybutadiene, *J. Polym. Sci. B Polym. Phys.*, 17, 1197 (1979).
35. V. Raju, H. Rachapudy, W. Graessley, Properties of amorphous and crystallizable hydrocarbon polymers. IV. Melt rheology of linear and star-branched hydrogenated polybutadiene.*J. Polym. Sci. B Polym. Phys*., 17, 1223 (1979).
36. L.J. Fetters, D.J. Lohse , D. Richter , T.A. Witten, A. Zirkel, Connection between polymer molecular weight, density, chain imensions, and melt viscoelastic properties, *Macromol.*, 27, 4639 (1994).
37. H.A. Khonakdar, J. Morshedian, U. Wagenknecht, S.H. Jafari, An investigation of chemical crosslinking effect on properties of high-density polyethylene, *Polymer*, 2003, 44(15): 4301-4309.
38. M.A. Kennedy, A.J. Peacock, L. Mandelkern, Tensile properties of crystalline polymers: linear polyethylene, *Macromol*., 27, 5297 (1994).
39. M.A. Kennedy, A.J. Peacock, M.D. Failla, J.C. Lucas, L. Mandelkern, Tensile properties of crystalline polymers: random copolymers of ethylene, *Macromol*, 28, 1407 (1995).

40. O. Darras, R. Séguéla, Tensile yield of polyethylene in relation to crystal thickness, *J. Polym. Sci. B Polym. Phys*, 31, 759 (1993).
41. V. Gaucher-Miri, R. Séguéla, Tensile yield of polyethylene and related copolymers: mechanical and structural evidences of two thermally activated processes, *Macromol.,* 30, 1158 (1997).
42. S. Humbert, O. Lame, G. Vigier, Polyethylene yielding behaviour: What is behind the correlation between yield stress and crystallinity?, *Polymer*, 50, 3755 (2009).
43. R.J. Young, P.B. Bowden, J.M. Ritchie, J.G. Rider, Deformation mechanism in oriented high-density polyethylene, *J. Mater. Sci.*, 8, 23(1973).
44. P.J. Flory, D.Y. Yoon, Molecular morphology in semicrystalline polymers, *Nature*, 272, 226(1978).

Figure Captions

Figure 1. Schematic of the ultrasonic single screw extruder (a) and the photograph of its screw (b).

Figure 2. Barrel pressure before ultrasonic treatment zone (a) and ultrasonic power consumption (b) as a function of the ultrasonic amplitude during the extrusion of XHDPE of various degree of crosslinking at a flow rate of 7.5 g/min for SSE with (open symbols) and without (filled symbols) the die.

Figure 3. Gel fraction (a) and crosslink density (b) of the decrosslinked XHDPE from SSE with (open symbols) and without (filled symbols) the die as a function of the ultrasonic amplitude. The gel fraction and crosslink density of the XHDPE are also indicated.

Figure 4. The normalized gel fraction versus the normalized crosslink density of the decrosslinked 1% (a), 2% (b) and 4% (c) XHDPE. Dotted and dashed lines represent Horikx function fits to Eqs. (1) and (2), respectively.

Figure 5. Frequency dependence of the storage modulus of XHDPE and decrosslinked 1% (a), 2% (b) and 4% (c) XHDPE obtained from SSE with (open symbols) and without die (filled symbols) without and with ultrasonic treatment at various amplitudes at a temperature of 160^{o}C.

Figure 6. Frequency dependence of the loss modulus of XHDPE and decrosslinked 1% (a), 2% (b) and 4% (c) XHDPE obtained from SSE with (open symbols) and without (filled symbols) die without and with ultrasonic treatment at various amplitudes at a temperature of 160^{o}C.

Figure 7. Frequency dependence of the complex viscosity of XHDPE and decrosslinked 1% (a), 2% (b) and 4% (c) XHDPE obtained from SSE with (open symbols) and without (filled symbols) die without and with ultrasonic treatment at various amplitudes at a temperature of 160^{o}C.

Figure 8. Frequency dependence of the loss tangent of XHDPE and decrosslinked 1% (a), 2% (b) and 4% (c) XHDPE obtained from SSE with (open symbols) and without (filled symbols) the die without and with ultrasonic treatment at various amplitudes at a temperature of 160^{o}C.

Figure 9. Frequency dependence of the complex viscosity of the virgin HDPE (a), sol of 1% XHDPE (b), sol of the decrosslinked 1% (c) and 2% (d) XHDPE from SSE with die, and sol of decrosslinked 4% XHDPE from SSE without (e) and with (f) the die obtained at an amplitude of 10 μm at temperatures of 140, 150 and 160^{o}C. Dashed lines represent Cross model fits to Eqs. (4) and (5).

Figure 10. FTIR spectra of the 1%, 2% and 4% XHDPE (a) and decrosslinked 1%, 2% and 4% XHDPE from SSE with die at an amplitude of 10 μm (b).

Figure 11. Melting temperature (a) and crystallinity (b) of the decrosslinked XHDPE from SSE with (open symbols) or without (filled symbols) die as a function of the ultrasonic amplitude. Values for the virgin HDPE and XHDPE are also indicated.

Figure 12. Stress-strain curves of the XHDPE, decrosslinked 1% and 2% XHDPE from SSE with die and decrosslinked 4% XHDPE from SSE without die obtained at an amplitude of 10 μm.

Figure 13. Young's modulus (a), yield stress (b), strain at break (c), and stress at break (d) of the decrosslinked XHDPE from SSE with (open symbols) and without (filled symbols) die as a function of the ultrasonic amplitude. Values of the HDPE and XHDPE are also indicated.

Table captions

Table 1. Maximum and minimum value of decrease of the crosslink density of decrosslinked 1%, 2% and 4% XHDPE.

Table 2. Cross model parameters and activation energy for flow of HDPE and sols of decrosslinked XHDPE

Table 1. Maximum and minimum value of decrease of the crosslink density of decrosslinked 1%, 2% and 4% XHDPE.

Material	$\Delta\nu_{max}$, Kmole/m^3	$\Delta\nu_{min}$, Kmole/m^3
Decrosslinked 1 %XHDPE	1.02×10^{-2}	6.46×10^{-3}
Decrosslinked 2 %XHDPE	1.13×10^{-1}	1.06×10^{-1}
Decrosslinked 4 %XHDPE	4.17×10^{-1}	4.05×10^{-1}

Table 2. Cross model parameters and activation energy for flow of HDPE and sols of decrosslinked XHDPE

Material	Die attatched	Amplitude, μm	A, Pa*s	T_b, K	τ, Pa	n	E, kJ/mol
HDPE	No	No	0.3823	3259	3.15×10^5	0.28	27.1
Sol of 1% XHDPE	No	No	0.0029	4864	6.60×10^3	0.56	40.4
Sol of decrosslinked 1 %XHDPE	Yes	10	0.5350	4652	3.61×10^3	0.42	38.7
Sol of decrosslinked 2%XHDPE	Yes	10	0.0562	4128	3.71×10^3	0.51	34.3
Sol of decrosslinked 4%XHDPE	No	10	0.0075	3764	6.43×10^3	0.67	31.3
Sol of decrosslinked 4%XHDPE	Yes	10	0.0038	4092	4.0×10^3	0.59	34.02

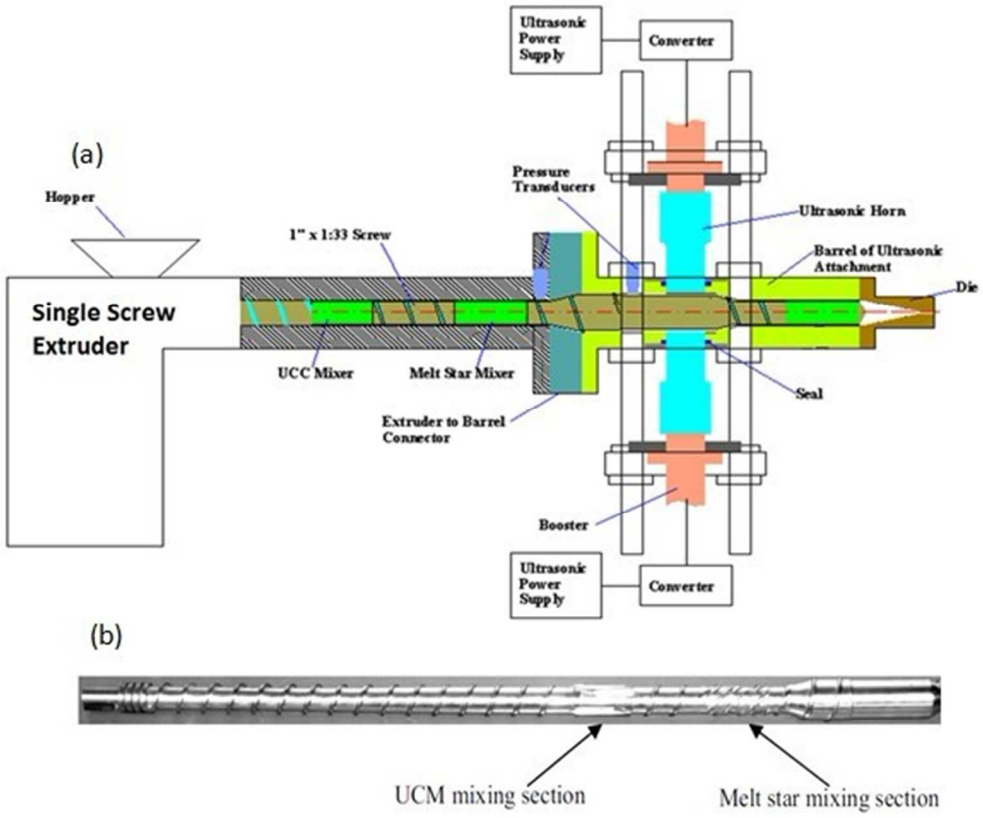

Figure 1. Schematic of the ultrasonic single screw extruder (a) and the photograph of its screw (b).
155x128mm (96 x 96 DPI)

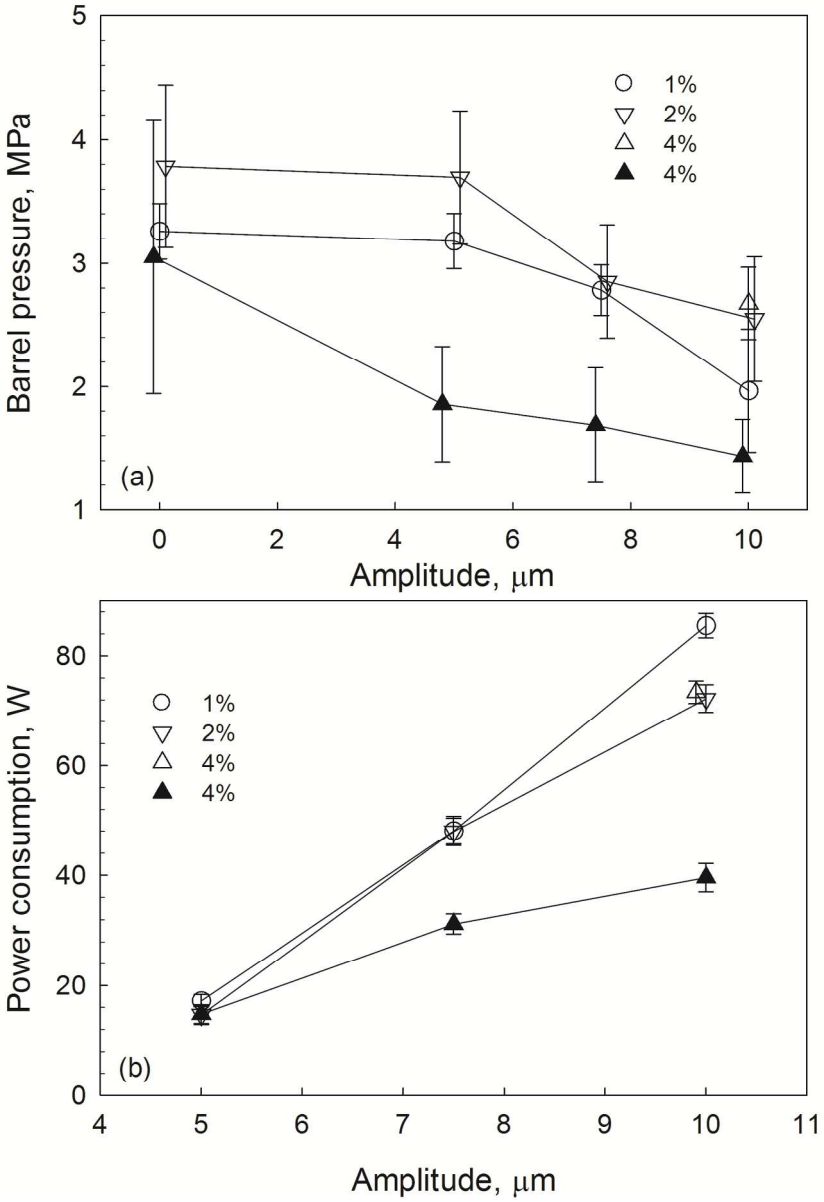

Figure 2. Barrel pressure before ultrasonic treatment zone (a) and ultrasonic power consumption (b) as a function of the ultrasonic amplitude during the extrusion of XHDPE of various degree of crosslinking at a flow rate of 7.5 g/min for SSE with (open symbols) and without (filled symbols) the die.
147x215mm (300 x 300 DPI)

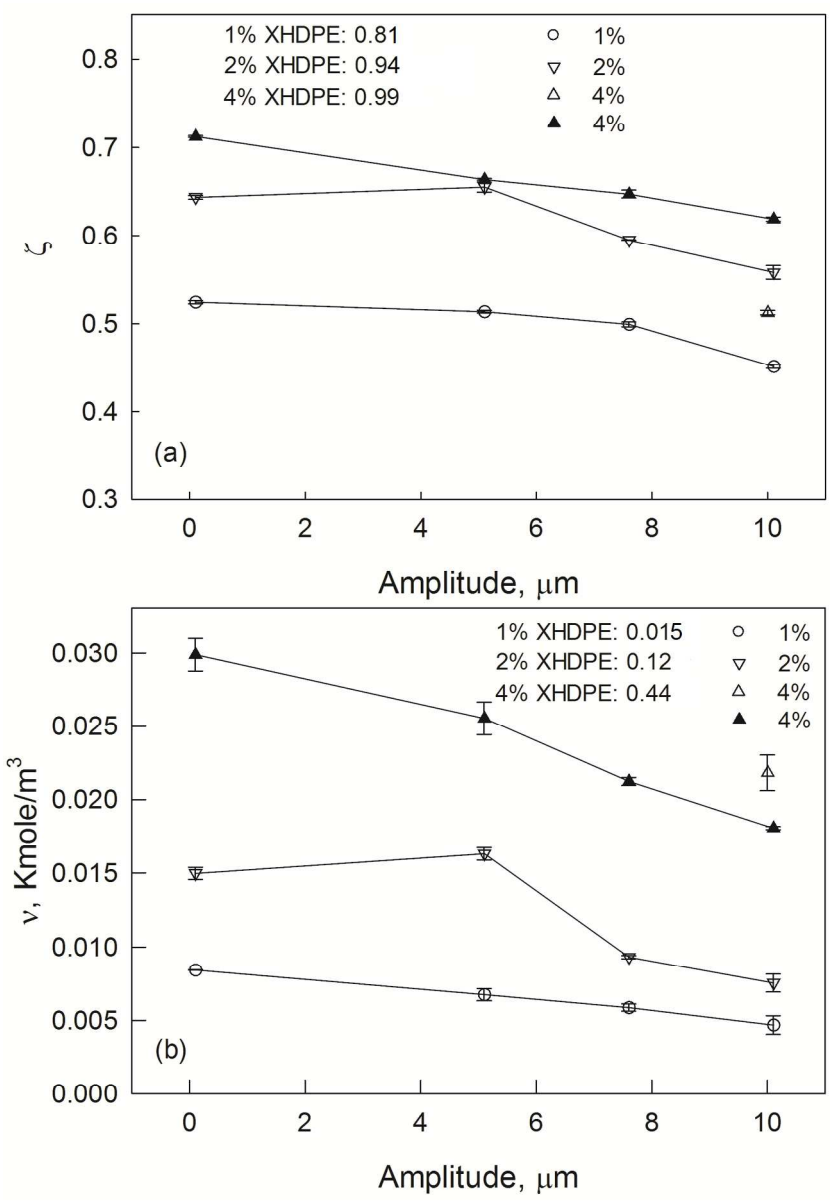

Figure 3. Gel fraction (a) and crosslink density (b) of the decrosslinked XHDPE from SSE with (open symbols) and without (filled symbols) the die as a function of the ultrasonic amplitude. The gel fraction and crosslink density of the XHDPE are also indicated.
382x549mm (120 x 120 DPI)

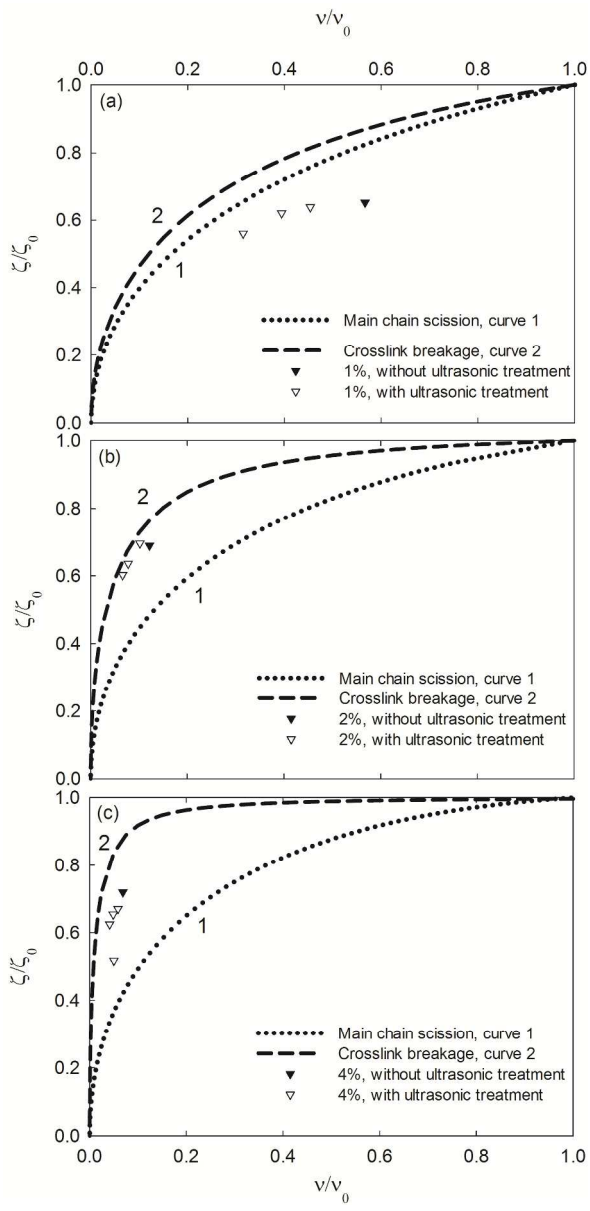

Figure 4. The normalized gel fraction versus the normalized crosslink density of the decrosslinked 1% (a), 2% (b) and 4% (c) XHDPE. Dotted and dashed lines represent Horikx function fits to Eqs. (1) and (2), respectively.
154x315mm (300 x 300 DPI)

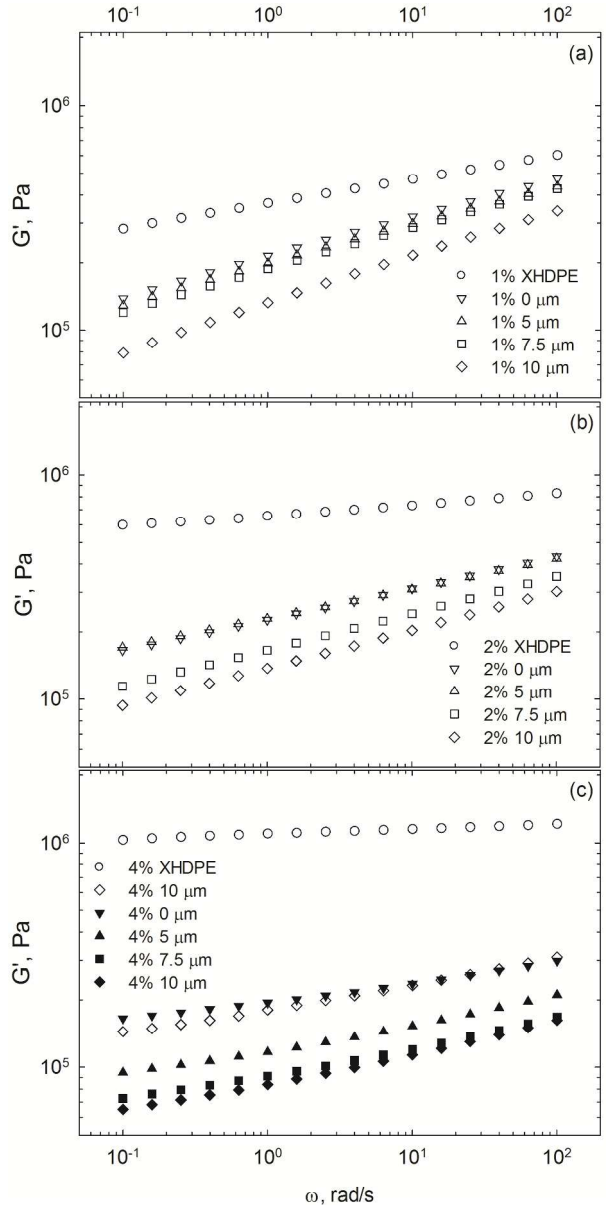

Figure 5. Frequency dependence of the storage modulus of XHDPE and decrosslinked 1% (a), 2% (b) and 4% (c) XHDPE obtained from SSE with (open symbols) and without die (filled symbols) without and with ultrasonic treatment at various amplitudes at a temperature of 160oC.
145x292mm (300 x 300 DPI)

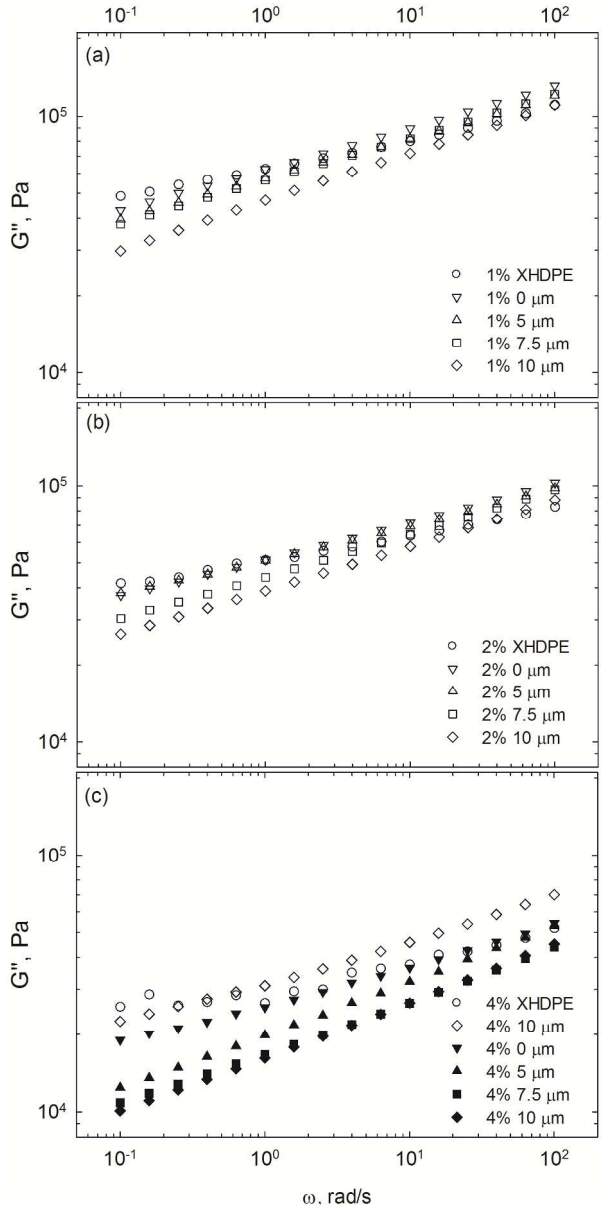

Figure 6. Frequency dependence of the loss modulus of XHDPE and decrosslinked 1% (a), 2% (b) and 4% (c) XHDPE obtained from SSE with (open symbols) and without (filled symbols) die without and with ultrasonic treatment at various amplitudes at a temperature of 160oC.
146x292mm (300 x 300 DPI)

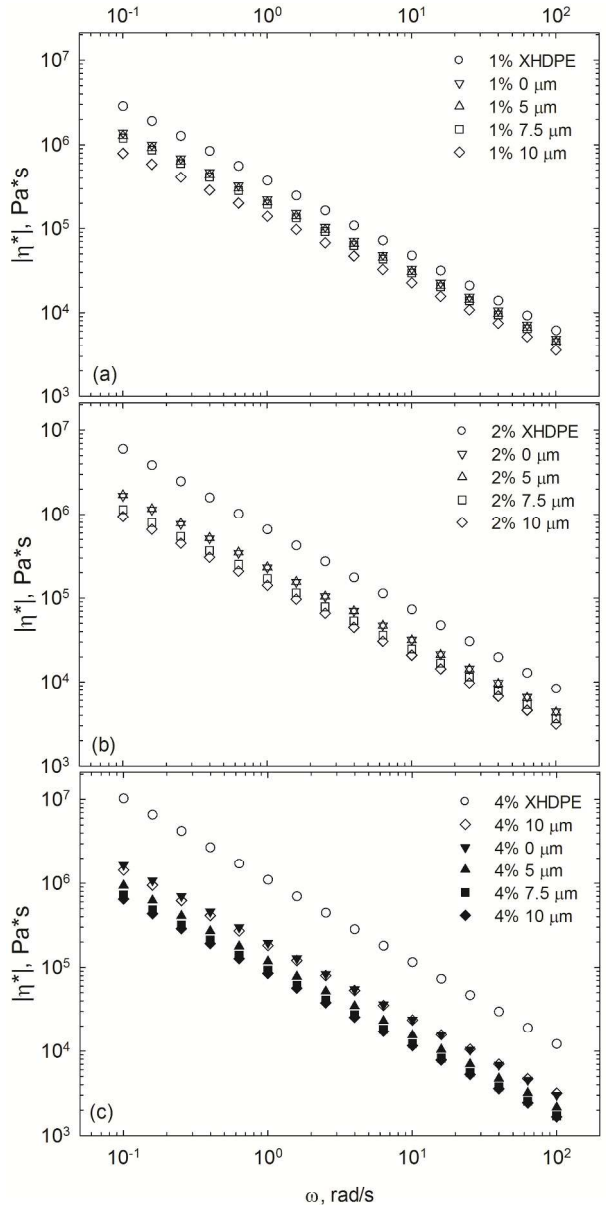

Figure 7. Frequency dependence of the complex viscosity of XHDPE and decrosslinked 1% (a), 2% (b) and 4% (c) XHDPE obtained from SSE with (open symbols) and without (filled symbols) die without and with ultrasonic treatment at various amplitudes at a temperature of 160oC.
146x293mm (300 x 300 DPI)

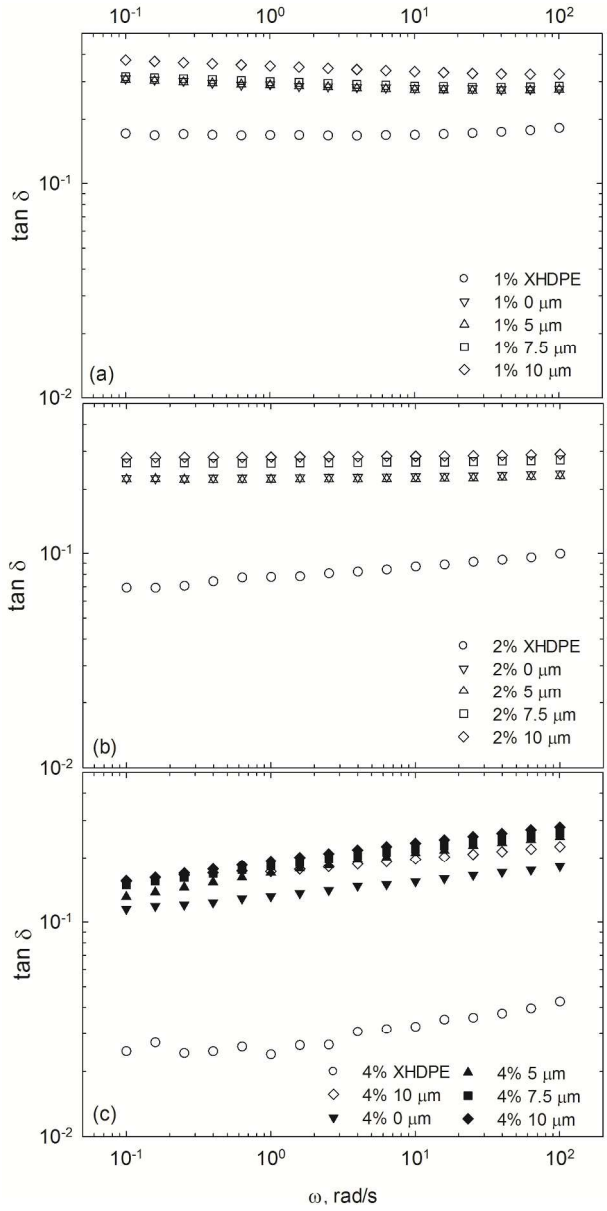

Figure 8. Frequency dependence of the loss tangent of XHDPE and decrosslinked 1% (a), 2% (b) and 4% (c) XHDPE obtained from SSE with (open symbols) and without (filled symbols) the die without and with ultrasonic treatment at various amplitudes at a temperature of 160oC.
148x292mm (300 x 300 DPI)

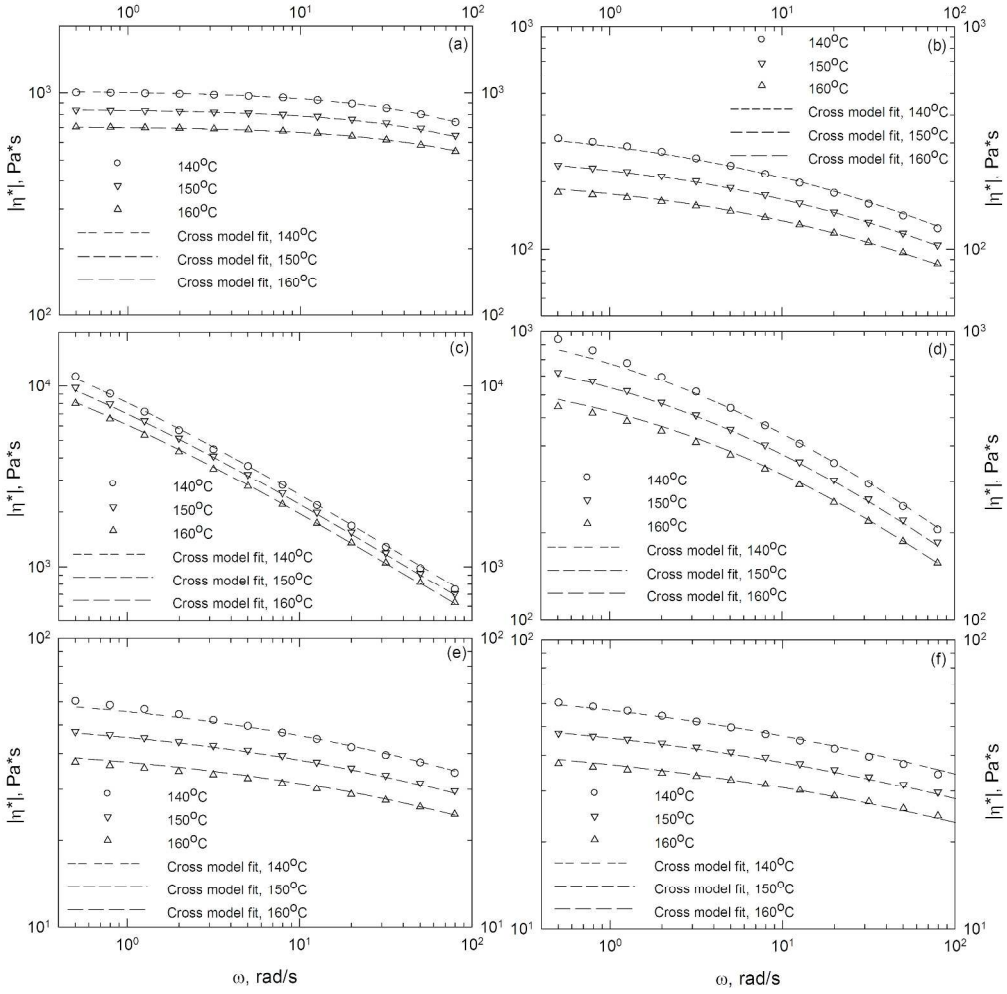

Figure 9. Frequency dependence of the complex viscosity of the virgin HDPE (a), sol of 1% XHDPE (b), sol of the decrosslinked 1% (c) and 2% (d) XHDPE from SSE with die, and sol of decrosslinked 4% XHDPE from SSE without (e) and with (f) the die obtained at an amplitude of 10 μm at temperatures of 140, 150 and 160oC. Dashed lines represent Cross model fits to Eqs. (4) and (5).
307x311mm (300 x 300 DPI)

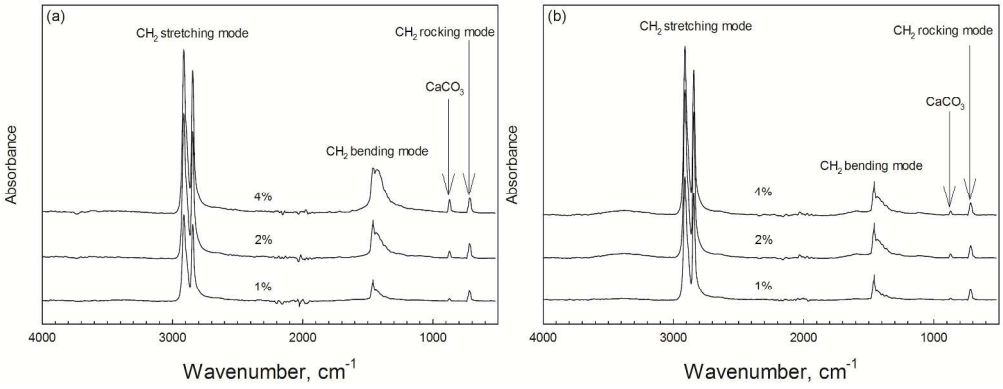

Figure 10. FTIR spectra of the 1%, 2% and 4% XHDPE (a) and decrosslinked 1%, 2% and 4% XHDPE from SSE with die at an amplitude of 10 μm (b).

278x107mm (300 x 300 DPI)

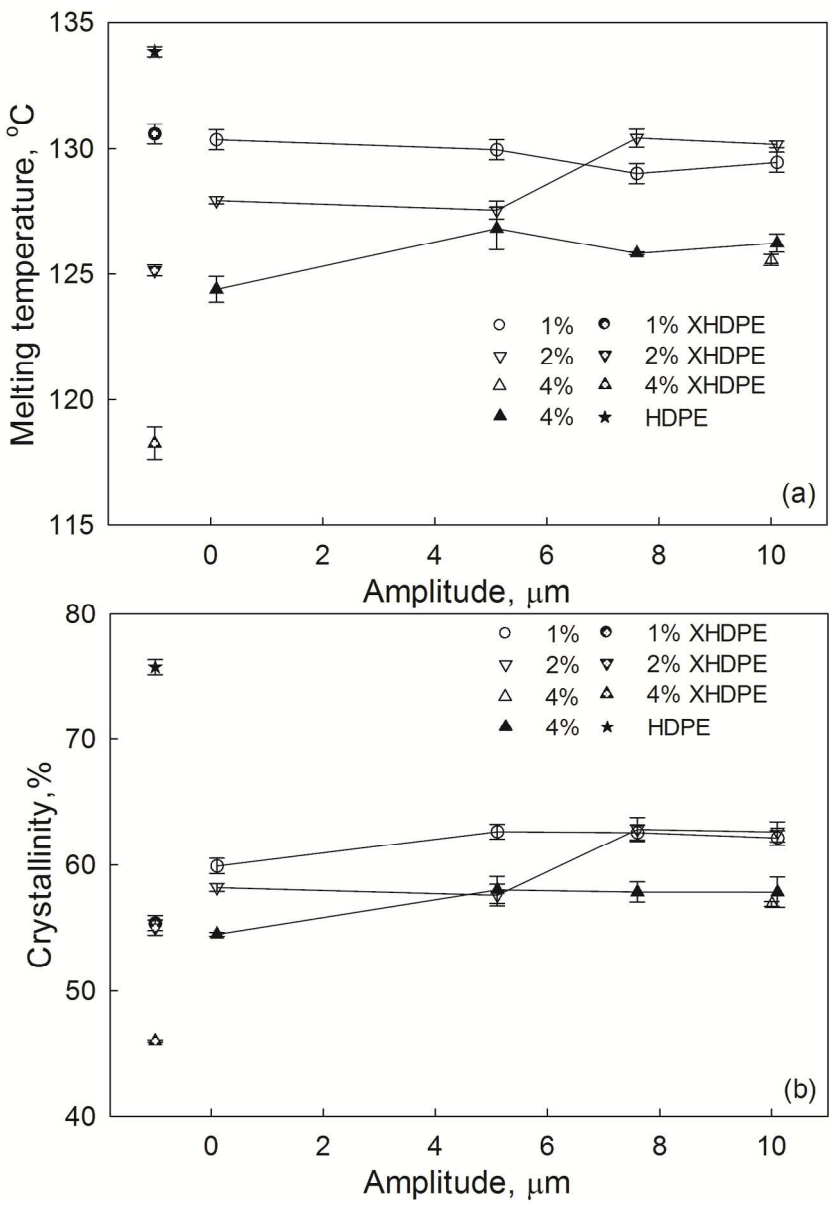

Figure 11. Melting temperature (a) and crystallinity (b) of the decrosslinked XHDPE from SSE with (open symbols) or without (filled symbols) die as a function of the ultrasonic amplitude. Values for the virgin HDPE and XHDPE are also indicated.
149x212mm (300 x 300 DPI)

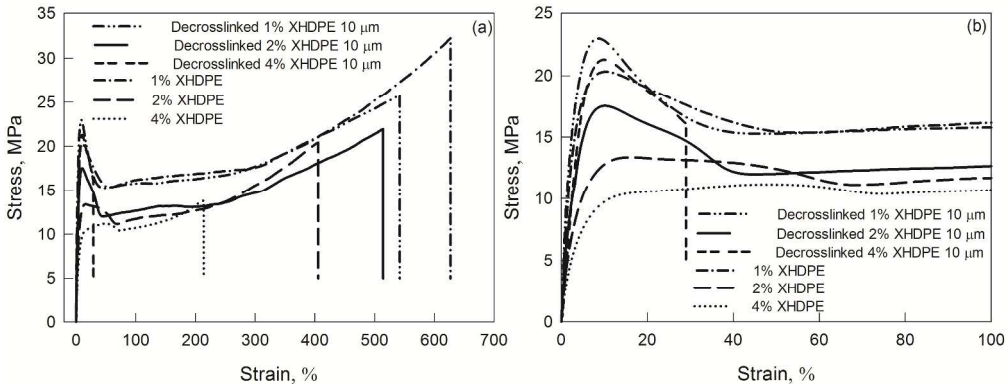

Figure 12. Stress-strain curves of the XHDPE, decrosslinked 1% and 2% XHDPE from SSE with die and decrosslinked 4% XHDPE from SSE without die obtained at an amplitude of 10 μm.
295x113mm (300 x 300 DPI)

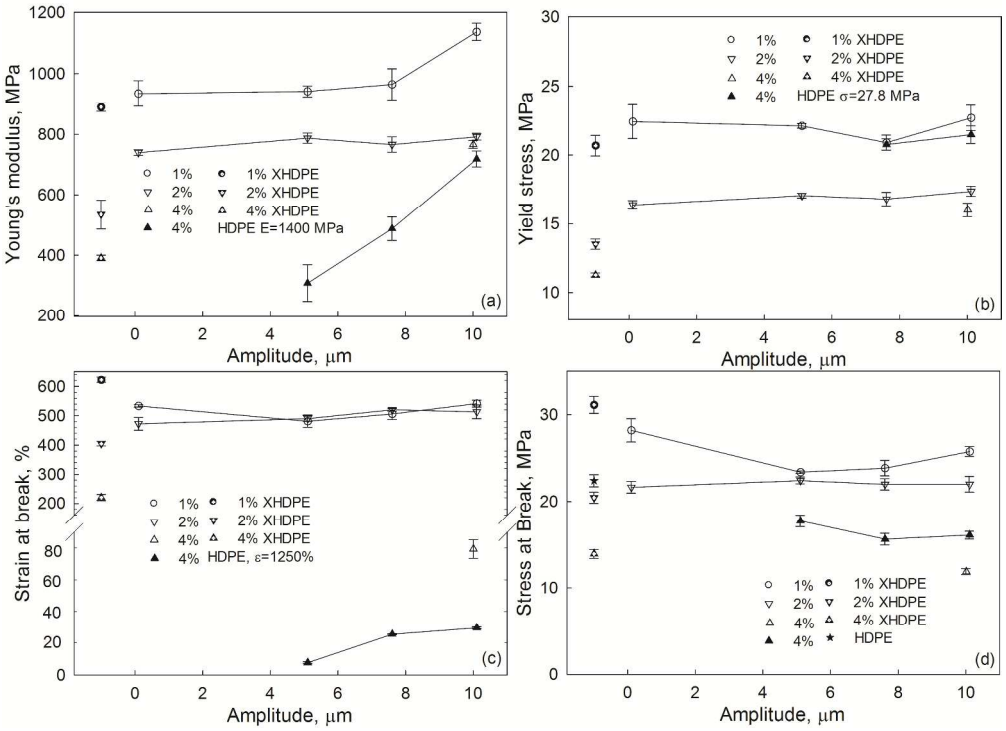

Figure 13. Young's modulus (a), yield stress (b), strain at break (c), and stress at break (d) of the decrosslinked XHDPE from SSE with (open symbols) and without (filled symbols) die as a function of the ultrasonic amplitude. Values of the HDPE and XHDPE are also indicated.
292x213mm (300 x 300 DPI)